Underground Ventilation – Tukkaraja (Ed)

Importance of using real-time and microscopic analysis techniques to characterize DPM in underground mines

A.A. Habibi
Ventilation Expert, PT Freeport Indonesia

K.O. Homan
Associate Professor, Missouri University of Science and Technology, MO, USA

A.D. Bugarski
Pittsburgh Mining Research Division, National Institute for Occupational Safety and Health, Pittsburgh, Pennsylvania, USA

ABSTRACT: Diesel equipment exhaust is a primary source of carbon-rich submicron particles in the underground mine atmosphere. In this study, the characterization of the morphological and physical properties of particles was used for identification of emission source and understanding the effect of diesel particulate matter (DPM) controll strategies on DPM characteristics. The size distributions and other physical properties of diesel aerosol were investigated on size-segregated samples collected in an underground mining operation. Scanning transmission electron microscopy (STEM) and fast mobility particle sizer were used concurrently to investigate size distribution based on particle projected area and electrical mobility. Other morphological attributes, such as fractal dimension, carbon net counts, and primary particle dimensions were examined for light and heavy-duty equipment powered by for various engine sizes. The results of STEM analysis showed presence of three types of chain-like agglomerates as well as volatile carbon particles. The results showed that when used concurrently, real-time and microscopic techniques can provide a wealth of information on characteristics of aerosols in underground atmosphere.

1 INTRODUCTION

Diesel engines are the main source of carbon-rich submicron aerosol in underground mines. Other sources of carbon-rich aerosols are oil mist from drilling operations, cigarette smoke, and suspended carbonate dust in ore (Zielinska et al., 2002; McDonald et al., 2003; Noll et al., 2006). Diesel aerosols are classified in three modes: nucleation mode (3-30 nm), accumulation mode (30-500 nm), and coarse mode (>500 nm) (Kittelson et al. 1998). Due to small size, the nucleation mode aerosols contribute substantially to number concentrations, but marginally to the particle total mass (Bugarski et al., 2012). In the U.S., the Mine Safety and Health Administration (MSHA) limits exposure of underground metal and nonmetal miners to diesel particulate matter (DPM) to 160 $\mu g/m^3$ of total carbon (TC) (30 CFR 57.5060). The TC concentrations are determined using NIOSH Method 5040 (NIOSH 2016). The mining industry implemented various engineering controls and technologies to reduce the exposure (Bugarski et al. 2014, Bugarski et al. 2022). A detailed knowledge of the size, structure, morphology, fractal dimension, and composition could be used to identify the sources and processes guiding formation, transformation of diesel aerosols. The same knowledge can be used for identifying effective control strategies and technologies, source apportionment, and to understand the interaction between micron-size dust particles and DPM.

In order to achieve the objectives, size segregated sampling using a multi-stage impactor with Transmission Electron Microscopy (TEM) grids was conducted. The sampling was

DOI: 10.1201/9781003429241-13

conducted during different mining operation phases to collect a range of diverse samples. Additionally, interaction of dust and diesel agglomerates can be investigated using Energy Dispersive Spectroscopy (EDS) and microscopic image analysis.

2 METHODOLOGY

2.1 *Instrumentation*

Real time instrumentation (Table 1) was used to measure the particles size distributions and number concentrations based on aerodynamic mobility (ELPI). The Electrical Low Pressure Impactor (ELPI+) was used to collect size-segregated samples for S/TEM analysis (Table 1).

Table 1. List of instrumentation used in the study.

Instrument or Device	Measurement or Sampling Objective
Electrical Low Pressure Impactor (Dekati, ELPI), (ELPI used for real time readings)	Continuous measurement of number concentrations and size distributions of aerosols with aerodynamic diameters between 30 and 10,000 nm
Electrical Low Pressure Impactor (Dekati, ELPI +) (ELPI+ is a newer model and was used to collect S/TEMgrid samples)	Collection of size-segregated samples for S/TEM

2.2 *S/TEM sample preparation*

The TEM grids were prepared by taping the grids on the aluminum foil and/or on a filter of the Dekati ELPI+ substrate. Samples were collected on carbon-coated TEM copper grids of 200, 300, and 400 mesh. These grids have a Formvar film support that prevented shaking during specimen preparation. Grid removal was challenging as there were multiple grids on the foils as shown in Figure 1a. Preparing the samples involved multiple steps. In order to reduce the particle bouncing, the aluminum foils were greased. Once grease was applied to the foils in the stencil, the foils were ready to be placed on the collection substrate. At this stage, the TEM grids already had been taped to the foil. The collection plate holder held the foil on the substrate, which sat on the jet plate. The cleaning process was a tedious task after each measurement. In order to facilitate the sampling process, spare set of substrates, TEM grids were prepared on surface and replaced underground during the test. Figure 1b shows this process. Sampling time was kept short (30 seconds to 60 seconds) to avoid overloading substrates and overlapping of particulate matter on the TEM grids and the consequent adverse impact on microscopic analysis.

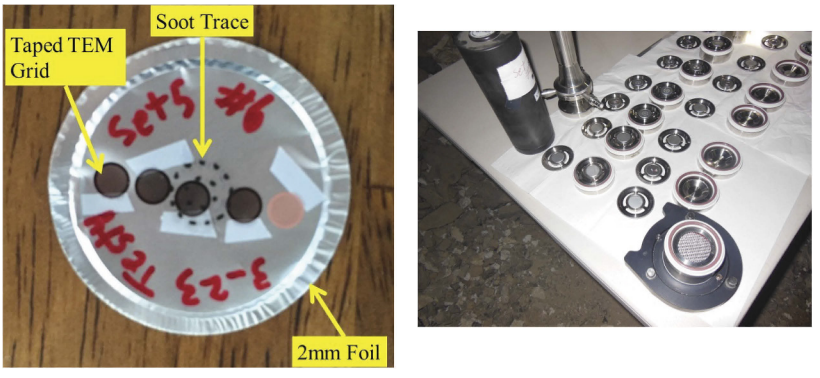

(a) (b)

Figure 1. A) S/TEM sampling grids taped on the 25-mm aluminum foil. The soot traces are visible. b) ELPI+ components disassembled for exchanging the substrates between the tests.

2.3 *Sample collection*

The measurements and sampling were conducted downwind of a 300m long active work zone shown in Figure 2. The measurement and sampling station was located between of the point where four ventilation drifts merged and the flow regulator.

The total flowrate through the zone was 26 – 33 m^3/s (55,000 – 70,000 cfm). During the measurement and sampling periods, the type of vehicles and corresponding activities were logged. During that period, the relatively large number of light-duty (LD) vehicles was used to deliver material and manpower . The heavy-duty (HD) equipment which was concurrently used in the work zone is listed in Table 2.

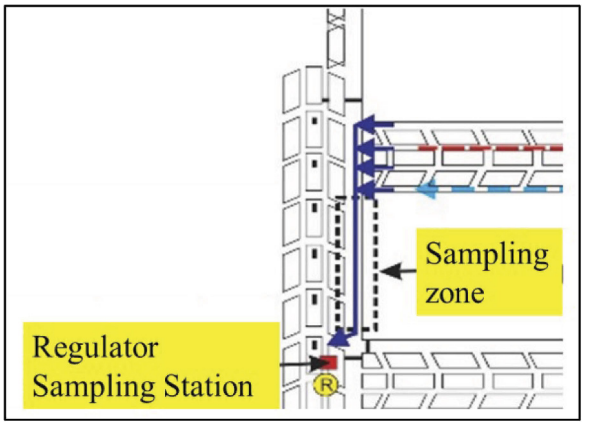

Figure 2. Schematic of work zone and measurement/sampling station.

Table 2. List of HD diesel equipment.

#	Equipment Manufacturer	Equipment Type	Equipment Type 2	EPA Tier	Engine Manufacturer and Model	Control Strategy
1	Wagner	LHD	HD Permissible	Pre	CATERPILLAR 3306 PCNA	Disposable Filter Element (Donaldson P60451)
2	Fletcher	Shield hauler	HD Non-Permissible	3	CUMMINS QSB6.7	Active Regeneration
3	Fletcher	Shield hauler	HD Non-Permissible	3	CUMMINS QSB6.7	Active Regeneration
4	Sandvik	LHD	HD Permissible	2	CATERPILLAR 3126B HEUI	Disposable Filter Element (Donaldson P60451)
5	Eimco	LHD	HD Non-Permissible	3	CUMMINS QSB4.5	DOC
6	Eimco	LHD	HD Non-Permissible	Pre	CATERPILLAR 3306 ATAAC	No Filteration

The ELPI was used for continuous real-time monitoring of number concentrations and size distribution of aerosols caried by ventilation air to the measurement/sampling station. Concurrently, the ELPI+ was used collect the size segregated samples for S/TEM and EDS analyses. The sampling station set-up are shown in Figure 3 a and 3b.

3 RESULTS AND DISCUSSION

The results from six tests were used to study the impact of equipment activities on the aerosols number and size distributions. The vehicle log showed that the exhaust of the over 35 LD and 6 HD vehicles contributed to the aerosols concentrations. The filtration system consisted of

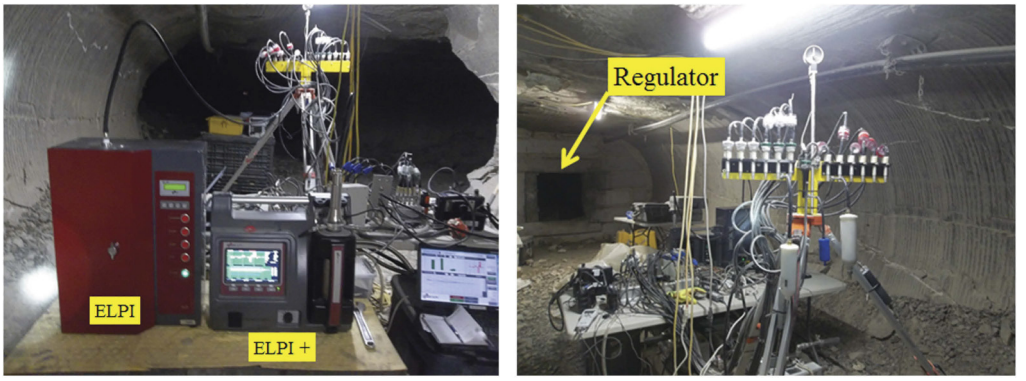

(a) (b)

Figure 3. Sampling station set-up. a) ELPI and ELPI+, b) Sampling station.

DFEs, tier 3 engine with diesel oxidation catalyst convertor (DOC) and tier 3 engine with active regeneration system (SMF-AR). Number and mass concentration measurements

The number and mass concentration of aerosols were measured by ELPI instrument. The results are for all six tests are shown in Figure 4. The number and mass concentrations fluctuated substantially during all periods. This appears to be the consequence of diversity in the tasks performed by the HD and LD equipment. During Test 1, two HD pieces of equipment retrofitted with SMF after treatment systems and several LD equipment were used most heavily. As shown in Table 2, the sixe HD vehicles included those with DFP filtration systems and SMF-AR. The high mass concentrations of predominantly micron size aerosols is attributed to high activity of the SMF-equipped vehicles that exhausted relatively low number concentrations of submicron aerosols but entrained substantial quantities of micron-sized dust. The results for test 2 – 6 show the relatively higher number concentrations of submicron aerosols along with proportionally high mass concentration of submicron aerosols primarily attributed to the diesel emissions of the HD and LD vehicles operated upwind and in the zone.

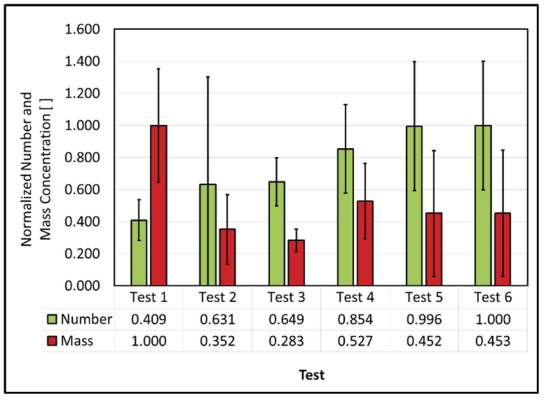

Figure 4. ELPI number and mass concentrations of aerosols measured.

3.1 *ELPI and S/TEM number and mass size distributions*

The results of SEM (Scanning Electron Microscopy) analysis show that the aerosols were distributed in two or three log-normal modes. The modes consisted of aged agglomeration mode

aerosols with count median diameters (CMD) ranging from 160 nm to 210 nm and freshly generated aerosols mainly in nucleation modes and partially in agglomeration modes with CMD ranging from 27 and 166 nm. The mechanically generated particulates (coarse particulate) contributed substantially less to number concentration compared to combustion generated aerosols. The number concentrations were noted to be higher when the diesel equipment was operated closer to the sampling station. During all six sampling periods, presence of aged aerosols transported from the outby areas was noted. The number distributions of aerosols at the sampling station represented a mixture of aged aerosols transported with ventilation air from outby areas and fresh aerosols generated in the zone. These distributions were mostly bimodal.

ELPI+ was used to collect TEM grids to conduct microscopic morphological and image analysis. Thirty-five samples were collected during six sampling periods. S/TEM analysis was conducted to obtain $D_{projected}$ for the collected agglomerates. The results show that size distribution obtained from S/TEM analysis are single modal and normally distributed. Three counts of coarse agglomerates (larger than 1um) were sampled.

The mass size distributions were dominated by entrained dust generated by movement of diesel-powered and battery powered equipment. The mass median diameter (MMD) ranging from 2.6 μm to 30 μm was measured. The Mass concentrations were mostly normally distributed except in two cases. The diesel particulates contributed to the second modes. In the case of coarse mode, the lognormal distribution was obtained by extrapolation and fitting the lognormal curves (Chimera Technologies 2009). Figure 5 shows the normalized mass size distribution during Test 6. The high spike at 2056 s was noted to be the result of entrained dust by an equipment operating close to the sampling station. Figure 5 a and b show size and mass distribution ELPI measurement and $D_{projected}$ STEM results.

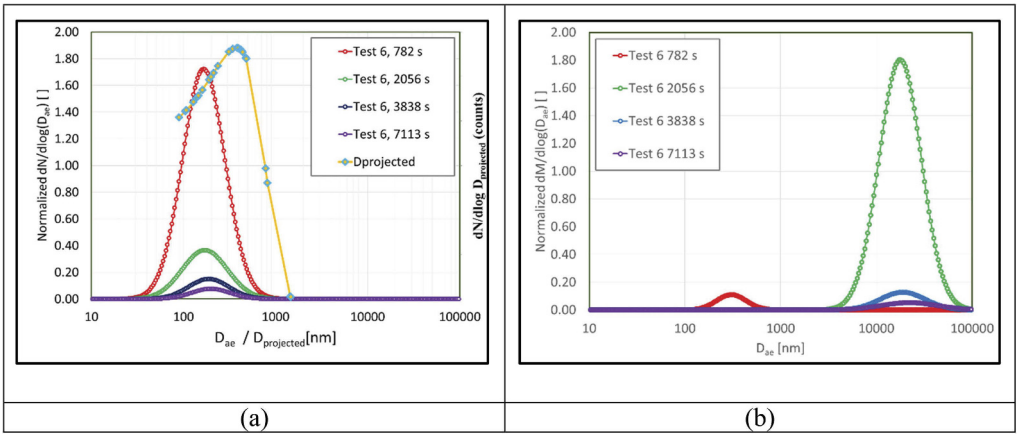

Figure 5. A) ELPI size distribution and Dprojected from STEM analysis. b) mass size distributions measured at the different instances during the Test 6.

3.2 *Fractal dimension and shape factor*

The fractal morphology of agglomerates collected during sampling was also analyzed. The samples were collected during six sampling periods in which conditions varied based on the engine operating conditions, accumulation and sampling conditions. In this study fractal dimension was calculated based on the maximum length (L_{max}). Figure 6 show the fractal dimension. Fractal dimension is represented by the slope of power relationship between number of primary particles in the agglomerates versus L_{max}/d on the logarithmic scale. Suggested values by Oh and Sorenson (1997) were used to account for the primary particles overlapping parameter (d), values of a=1.19 and k_α = 1.81 used. Koylu et al. (1995) suggested values of a=1.09 and k_α = 1.21 to calculate the fractal dimension for the agglomerates. The results show that the fractal dimension vary from 1.87 to 2.04 which is higher than what was calculated in the sampling zone (except in the case where LHD was intentionally measured

without DFE). These results therefore show that larger entrained particles and aged agglomerates have contributed to larger fractal dimensions.

Shape factor is used to describe the agglomerates elongation. If shape factor is close to 1.0, it indicates that the agglomerates are spherical, where 0.1 shape factor is an indicative of long-chained or elongated agglomerates (Nord et al., 2004; Mustafi and Raine, 2009). The results show a majority of agglomerates with shape factor of higher than 0.5. Figure 6 (a) and (b) show the results for fractal dimension and shape factor.

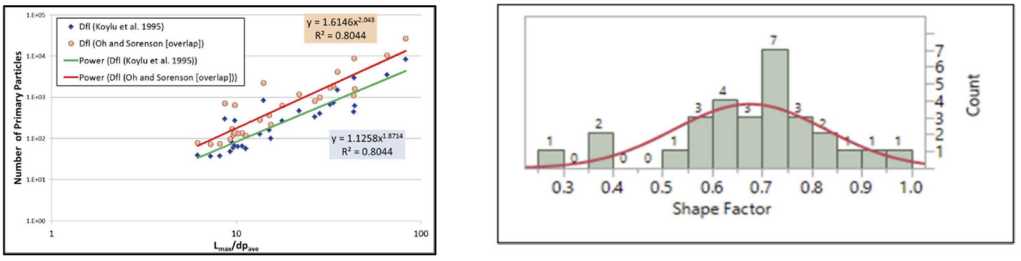

(a) (b)

Figure 6. A) Fractal dimension of aerosols b) Results of shape factor analysis.

3.3 *Carbon-rich primary particle types*

S/TEM image analysis was conducted on 290 agglomerates collected using the ELPI+ muti-stage impactor. The results showed that 78 percent of analyzed agglomerates (227 counts) had primary particle with graphitic layered (onion shell) structure as in Figure 7 (a). Another 12 percent (35 counts) of agglomerates had chain-like agglomerates with amorphous carbon-rich primary particles as in Figure 7 (b). In addition, 10 percent (28 counts) of agglomerates were chain-like agglomerates with small catalyst particles attached to primary particles. We observed that some of the agglomerates had one carbon rich primary particles where others had multiple nuclei centers. This could be due to the combustion process during which they were formed. Chen et al. (2005) explains the generated primary particle nuclei centers during post-combustion processes could increase in size by condensation of volatile compounds. They further explained that primary particles could collide with others during accumulation mode to form larger agglomerates.

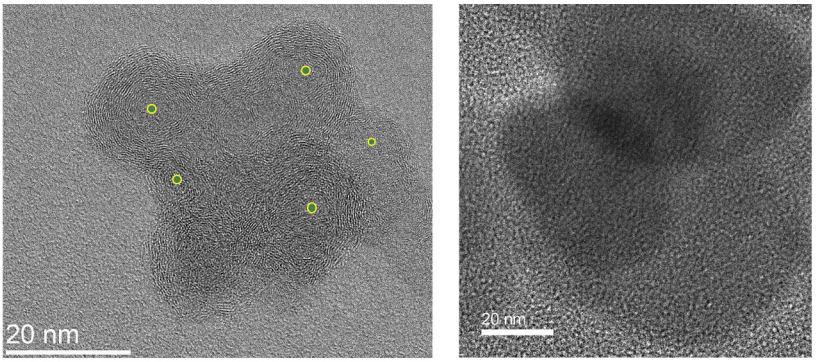

(a) (b)

Figure 7. TEM BF image of primary particles (a) with graphitic structure with multiple nuclei centers and (b) amorphous structure.

The diameter of carbon-rich primary particles d_p are normally distributed for agglomerates with graphitic structure with mean value of 23.6 nm and s = 6.3 nm and for the agglomerates with catalyst with mean value of 24.2 nm and s = 6.2 nm. The d_p agglomerates with amorphous structure were bi-modal.

3.4 *S/TEM analysis of volatile agglomerates and EDS results*

Primary particles emitted from combustion engines can be categorized into two types: volatile, and solid particles (Mathis et al. 2004). Morphological analysis at the interface of dust and DPM particles show some volatile agglomerates attached to stable solid particles. The larger agglomerates were observed at the higher stages of ELPI+. EDS analysis results depicts non-diesel volatile interface where particles evaporated after exposure to electron beam for 20 seconds, as shown in Figure 8 c and d. The larger chain-like agglomerate (Figure 8 a, agglomerate #2) seemed more stable than the smaller of the two (Figure 8 a, agglomerate #1).

The morphological and EDS analysis results were also used to identify the source of each particle. The SE (Figure 8b) image showed that the larger particle is thicker and denser compared to agglomerates #1 and #2. The EDS results indicate the large agglomerate contains high counts of Sodium (Na) and low counts of Potassium (K), Magnesium (Mg), Aluminum (Al), Silicon (Si). The source of Sulfur (S) and Fe is likely from lubricating oil and diesel fuel.

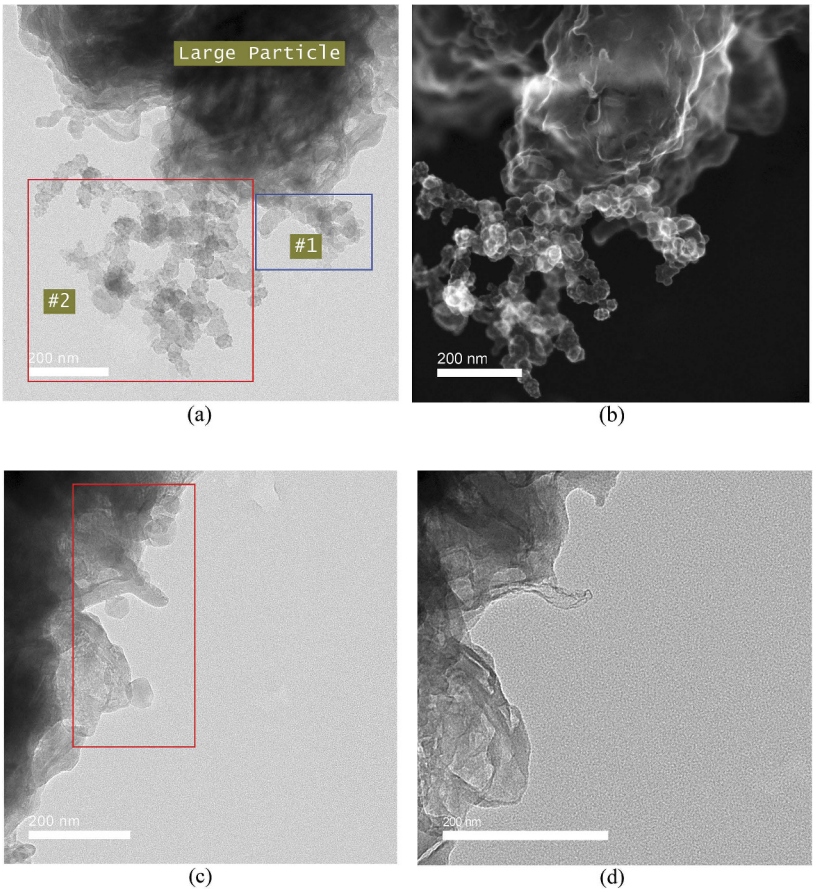

Figure 8. S/TEM image analysis a) STEM BF of particles at 400K magnification b) SE image of particles at 300K magnification c) STEM BF of volatile interface at time 0 second d) STEM BF of volatile interface at time lag 20 seconds.

The EDS results show agglomerate #2, is carbon rich. Traces of Na and Si did not continue to agglomerate #2 unlike S. The EDS result for agglomerate #1 showed the trace of S net counts was insignificant, unlike agglomerate #2. Similarly, the Si, Al, Mg and Na net counts were either similar or slightly lower in agglomerate #1. This suggests that agglomerate #1 was carbon-rich, volatile, and from a different source than #2. The morphological S/TEM analysis of the particles mentioned above showed a graphitic structure for the primary particle of chain-like agglomerate #2. However, an amorphous structure was observed for primary particles in agglomerate #1.

The TEM and SE images of agglomerate #2 show small particles on the primary particles. The EDS results indicate Na and S elements surrounding the primary particles. The diameter of primary particles for agglomerate #2 ranged from 23 nm to 50 nm. For agglomerate #1, the primary particles appear to be smaller than 30 nm. Agglomerate #2 with the L_{max} of 642.81 nm, width of 379.65 nm and calculated SF of 0.59 seemed to have similar characteristics to the samples collected in sampling zone. Agglomerate #2 therefore appears likely to be a product of the diesel combustion process from equipment in the sampling zone. The attached Na particles represent the dust in the uncontrolled zone whereas S is likely to be from the engine. As for agglomerate #1, projected measurements were difficult to obtain as some of the volatile primary particles evaporated while EDS mapping was underway. However, the combined results and observations of morphological and EDS mapping make it likely that agglomerate #2 did not have a combustion source.

4 CONCLUSION

The present study was designed to evaluate importance of monitoring and sampling the aerosols emitted by diesel-powered equipment performing multiple tasks in the section of underground mine. The study showed that entrainment of the micron sized dust due to movement of diesel-powered equipment is the primary contributor to mass concentrations of particulates at the section. The mass median diameter of entrained dust was found to range between10 μm to 30 μm. The dominant sources of the submicron aerosols were various types of LD and HD diesel-powered equipment. Diesel aerosols were found to be distributed between nucleation and agglomeration modes. We observed that fresh aerosols were distributed in single mode and aged aerosols were distributed bimodaly.

The electron microscopy analysis of size segregated aerosols samples revealed that diesel aerosols agglomerates consist of three types of carbon-rich primary particles. with the majority of those are made of carbon-rich primary particles with graphitic structure. The smaller part is made of carbon-rich primary particles with amorphous structure or carbon-rich primary particles infused with catalyst. The diameter of primary particle with amorphous structure is bi-modally distributed.

The EDS results along with morphological attributes were used to investigate chemical composition of the fractal agglomerates attached to the micron size particles. EDS results show that the diesel chain-like agglomerates with high carbon to oxygen ratio and significantly low net counts of dust and mining environment elements such as Na, Si, Fe, K and S. Volatile chain-like agglomerates with amorphous primary particles seemed susceptible to beam damage. EDS results for these agglomerates showed high C net counts and equal or slightly lower Na, Si and K.

The EDS results show that the typical elements (Na, S either from fuel or not, Si) were observed in lower stages of ELPI+. The elements were observed at very low net counts during control zone test and higher net counts during regular mining activity due to the presence of dust. High C/O net counts ratio for chain-like agglomerates varied from 6.5 to 9.6. Most of the chain-like agglomerates appeared to have chain-like primary particles with graphitic structure.

The interaction of dust and volatile chain-like agglomerate was investigated at higher stages of ELPI+ multi-stage impactor. It was observed that amorphous carbon rich particles tend to be present at the interface of dust and chain-like agglomerates. The primary particles at the interface with large particles were sensitive to beam damage and evaporated during EDS mapping.

The sampling during mining activity provided valuable data to compare the results with controlled zone sampling and investigate: i. The interaction of carbon rich agglomerates at the interface with large dust particles. ii. The morphological differences between the agglomerates. iii. Investigate the volatile agglomerates observed during the sampling to determine the sources of agglomerates.

5 DISCLAIMER

The findings and conclusions in this manuscript are those of the authors and do not necessarily represent the official position of the National Institute for Occupational Safety and Health (NIOSH), Centers for Disease Control and Prevention (CDC). Mention of company names or products does not constitute endorsement by NIOSH or CDC.

REFERENCES

Bugarski, A.D., Janisko, S.J., Cauda, E.G., Patts, L.D., Hummer, J.A., Westover, C., Terrillion, T. 2014. Aerosols and criteria gases in an underground mine that uses FAME biodiesel blends. Ann. Occup. Hyg. 58(8):971–982. http://dx.doi.org/10.1093/annhyg/meu049.

Bugarski, A.D., Hummer, J.A., Vanderslice, S., Mischler, S. 2020. Contribution of various types and categories of diesel-powered vehicles to aerosols in an underground mine. Journal of Occupational and Environmental Hygiene 17: 121–134. https://doi.org/10.1080/15459624.2020.1718157.

NIOSH 2016. Monitoring diesel exhaust in the workplace. In: NIOSH Manual of Analytical Methods (NMAM), 5th Edition, Chapter DL, Cincinnati, OH: U.S. Department of Health and Human Services, Centers for Disease Control and Prevention, National Institute for Occupational Safety and Health. Available from: https://www.cdc.gov/niosh/nmam/pdfs/NMAM_5thEd_EBook.pdf. Accessed on July 2, 2022.

Zielinska B, Sagebiel J, McDonald J, Rogers CF, Fujita E, Mousset-Jones P (2002). Measuring diesel emissions exposure in underground mines: a feasibility study. Research directions to improve estimates of human exposure and risk from diesel exhaust, Special report. Boston: Health Effects Institute, pp. 181–232

Kittelson, 1998, D. B. Engines and nanoparticles: A review. J. Aerosol. Sci. 1998, 29 (5-6), 575–588.

Mathis, U., Kaegi, R., Mohr, M., Zenobi, R. (2004). TEM analysis of volatile nanoparticles from particle trap equipped diesel and direct-injection spark-ignition vehicles. Atmospheric Environment 38 (2004) 4347–4355

Nord, K., Haupt, D., Ahlvik, P., and Egeback, K.-E. (2004). Particulate Emissions from an Ethanol Fueled Heavy-Duty Diesel Engine Equipped with EGR, Catalyst and DPF, SAE Paper 2004-01-1987